Classical magnetoresistance of an antidot lattice

1993 J. Phys.: Condens. Matter 5 5623

(http://iopscience.iop.org/0953-8984/5/31/024)

J. Phys.: Condens. Matter 5 (1993) 5623–5636. Printed in the UK

Classical magnetoresistance of an antidot lattice

R W Tank and R B Stinchcombe
Department of Physics, 1 Keble Road, Oxford, OX1 3NP, UK

Received 25 March 1993, in final form 20 May 1993

Abstract. We undertake a theoretical study of an ideal lattice of circular hard wall antidots in a low magnetic field where classical skipping orbits can exist. We study the transmission of electrons through constrictions between antidots, and thence their paths through the lattice, which can take the form of a correlated random walk. Analytic expressions for the conductivity tensor are derived, and these give numerical values comparable with recent experiments.

1. Introduction

This paper provides a theoretical description of the magnetotransport properties of 'antidot' array structures.

The fabrication of semiconductor microstructures using molecular beam epitaxy, metal organic vapour phase epitaxy, focused ion beam techniques etc, has in the last few years provided great stimulus to experimental work on the fundamental properties of small electronic systems. Nanostructures, such as quantum dots (Reed 1988), and quantum wires (Roukes 1987), as well as layers, have shown a remarkable range of interesting behaviours, in capacitance and spectroscopic measurement (Smith 1988, Hansen 1989, Sikorski 1989, Lorke 1990), in susceptibilities, and in transport effects (Roukes 1987) with or without the presence of a magnetic field. Dot and antidot lattices are particularly interesting candidates for spectroscopic (Lorke 1992) and transport studies (Weiss 1991, Takahara 1991). They possess the features of isolated quantum dots, such as modified cyclotron resonance branches, and structure in the capacitance (Smith 1988), due to the confining potential and to the effect of the Coulomb interaction between small numbers of charges in the well. In addition they may show novel collective (Que 1988, Kern 1991) and single-particle effects; in particular, the levels found in a single dot become shifted and broadened due to tunnelling between dots (or antidot reservoirs) in a dot or antidot lattice, conductivity can range from hopping to band type, and may be caused to switch between the two types on changing carrier concentration by photoluminescence or by varying a gate voltage. While a simple intersection in the form of, for example, a cross-shaped constriction, gives rise to rich transmission behaviour (Ford 1990), a lattice of such constrictions can arise in quantum antidot systems, and thus have profound effects on transport, some of which are the subject of the present paper. New quantum interference effects occur, which are expected to be rich in structure. However, even at the classical level the interplay of classical orbit shape and constriction geometry leads to remarkable effects. This is the situation discussed in the present paper. The richest behaviour occurs when a magnetic field is present, which is the situation addressed here. Recent experiments have shown pronounced structure in the magnetoresistance of periodic antidot arrays (Ensslin 1990, Weiss 1991, Fang 1990, Sundaram 1992, hereafter denoted as I) which can be interpreted in part using the approach developed in the theoretical investigation given in this paper.

0953-8984/93/315623+14$07.50

The layout of this paper is as follows. Section 2 describes the classical electron orbits and their passage through a constriction in terms of the motion of orbit centres. Since a linear response approach will be used for the conductivity, the orbits are only needed in zero electric field. Section 2 begins with a description of the idealized model used for the antidot array. Section 3 provides a description of the current and includes an effective particle picture. Section 4 applies the description to the conductivity of the antidot lattice. In a typical low-scattering regime the orbit centres undergo a random walk through the antidot array. The characteristics of the walk, and hence of the magnetoconductivity, are determined by the properties discussed in section 2. Results for the conductivity as a function of field are given at the end of section 4. Section 5 briefly compares the result with experiment and provides a concluding discussion.

2. Classical electron orbits and passage through a constriction

2.1. Model

Our model for a real antidot array is a perfect square lattice (with lattice constant a) of identical antidots. A portion of such a lattice is shown in figure 1. In the model each antidot, of radius R, has an infinite hard wall with which the electrons collide elastically. Between the electrons the potential is constant. In addition we neglect altogether electron–electron interaction effects, and treat the electron motion classically. The classical approximation requires orbit radii much larger than quantum length scales. In the experiments reported in I the condition is weakly satisfied in the sense that, while the two scales are not very different, no quantum interference effects appear, and gross aspects of the conductivity appear to be captured by the approximation. Then the assumption of an infinite hard wall is not severe, since in semiclassical situations the main effect is the reflection at the classical turning point, rather than the orbit details near that point. The approximation of a perfect lattice is substantially correct for many real (finite) arrays, in particular the antidot array of I. However, as discussed in section 5, deviations from perfect periodicity may be important in particular regimes. In particular they are expected to be the reason for a threshold phenomenon seen in I. The neglect of electron–electron interactions is very difficult to justify, except in the cases of cyclotron resonance and Hall effect, where the Kohn theorem (Kohn 1961) and its extension (Stinchcombe 1974) applies, and then only for unconfined electrons or those in parabolic wells (Maksym 1990, Brey 1989). Section 5 discusses some possible effects excluded by the neglect of electron interactions in the present magnetotransport context.

We proceed to investigate the properties of the model. Taking the origin as the centre of an antidot, the electrons then reside in *reservoirs* centred on $((n_1+\frac{1}{2})a, (n_2+\frac{1}{2})a)$ (where n_1 and n_2 are integers) which are joined by *constrictions* of width $2l = a - 2R$. In the presence of a uniform perpendicular magnetic field the electrons will undergo cyclotron motion with radius r_c. In the regime where $l < r_c < a/\sqrt{2} - R$ electrons that are near to an antidot will perform a skipping orbit (Halperin 1982, Büttiker 1988, Prange 1968, Kosevich 1955) along the edge of that antidot (see figure 1).

The motion of an electron can always be described in terms of the motion of the centre of its cyclotron orbit. For a skipping electron, this *orbit centre* will step around the antidot, remaining at the same distance r from the antidot (see figure 1). The angle through which the orbit centre rotates in each step is

$$\phi(r) = 2\cos^{-1}\left(\frac{R^2+r^2-r_c^2}{2Rr}\right). \tag{1}$$

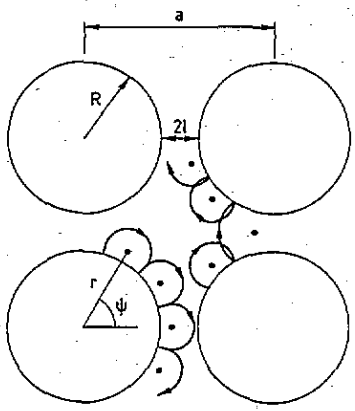

Figure 1. A portion of the antidot lattice containing four circular antidots. Two electrons are shown performing skipping orbits; one is reflected at a constriction and the other transmitted. The dots represent the successive positions of the orbit centres. Also shown is the radius r and phase ψ of an orbit centre.

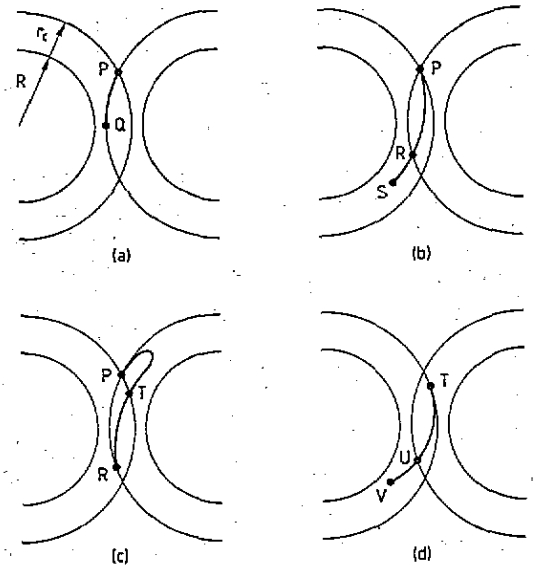

Figure 2. This series of diagrams shows the initial line of orbit centres and its first three evolutions. The inner circles are the edges of the antidots, which have radius R. The outer circles have radius $R + r_c$, the maximum orbit radius of a skipping electron.

2.2. *Passage of an orbit centre through a constriction*

On reaching a constriction a skipping electron will either be reflected by collisions with the neighbouring antidot, or be transmitted to the next reservoir (see figure 1). The outcome depends upon the 'radius' r and 'phase' ψ of the orbit centre, as we now discuss. Consider the line PQ of initial orbit centres shown in figure 2(*a*). The next position of these is the line PS shown in figure 2(*b*) (PS is the *first evolution* of the line PQ). The section of the line RS contains orbit centres that have now been transmitted. Consequently only the section PR need be considered for the next step or *second evolution*. Electrons with orbit centres on PR will collide with the neighbouring antidot and therefore the next position of their orbit centres will be given by rotation around that antidot.

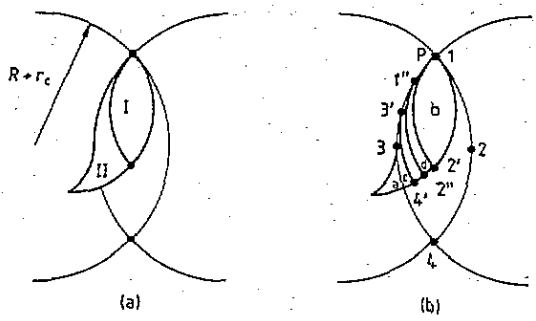

Figure 3. The initial area of orbit centres considered in the text. (*a*) Shows its division into regions I, (containing centres that are reflected), and II (containing centres that are transmitted). (*b*) Shows further subdivisions discussed in the text. The outer circles have radius $R + r_c$.

Figures 2(*c*) and 2(*d*) show the second and third evolutions of PQ. The line section PT is reflected and UV is transmitted.

2.3. Evolution of an initial area

Whether or not an orbit centre is transmitted or reflected depends not only on r but also on ψ. In order to cover all possibilities an initial *area* of orbit centres must be considered.

Figure 3(*a*) shows a suitable area, bounded by the line PQ and its first evolution. Electrons with orbit centres in area I are reflected and those with centres in area II are transmitted. We therefore have three distinct annular regions in which the orbit centre can lie They are:

A	$r_a < r < R + r_c$	electron is reflected
B	$r_b < r < r_b$	ψ-dependent transmission or reflection
C	$R - r_c < r < r_b$	electron is transmitted.

The dependence of r_a and r_b on the magnetic field will be needed later and is discussed at the end of this section.

It is possible to make further subdivisions of the initial area, and some of these are shown in figure 3(*b*). Electrons with orbit centres lying in region a are transmitted without ever colliding with the neighbouring antidot. Those with centres in region b are reflected after colliding once. Region b is bounded by the lines PR and 1–2′, where the line 1–2′ is given by the first *anticlockwise* (i.e. backwards) evolution of the line 1–2.

Similarly, electrons with centres in region c are transmitted after one collision with the neighbouring antidot. Region c is bounded by the lines 3–4 and 3′–4′, where 3′–4′ is the second anticlockwise evolution of the line 3–4. Furthermore, region d contains centres that are reflected after two collisions. Region d is bounded by 1–2′ and 1″–2″, where 1″–2″ is the third anticlockwise evolution of the line 1–2.

This divisioning can be continued indefinitely. As the boundary of I and II shown in figure 3(*a*) is approached, the number of collisions that the electron has in the constriction region continues to rise. In turn this means that the length of time that the electron spends there rises. An electron that spends a lot of time in the constriction is very likely to collide with any impurities there. Such a collision is just as likely to result in the electron being (eventually) transmitted or reflected. Thus the presence of impurities will have the effect of slightly widening the annular region B.

2.4. Results

When the subdivision of the initial orbit area shown in figure 3(*b*) is carried out, it is found that there is little difference between the third and fifth evolutions of PQ and practically no difference between the fifth and seventh. A similar result applies for the second, fourth and sixth evolutions. The boundary between the reflected and transmitted regions can be approximated by the fifth evolution of the line 1–2, and hence r_a and r_b can be obtained. It is found that r_a shows little variation with cyclotron radius whereas r_b shows a linear decrease with r_c.

It is far harder to find an approximation for f, the fraction of orbit centres in annulus B that are transmitted. An estimate of $f = 0.4$ was obtained by direct evaluation of areas in a diagram like figure 3(*b*). However, the results to follow are not very sensitive to the value of f.

2.5. Mixing of orbit centres at a constriction

An electron which experiences a collision with a neighbouring antidot will emerge with a different radius of orbit from that with which it came in. By symmetry under reversal of the magnetic field, a reflected orbit can only emerge within annuli A or B, and a transmitted one can only emerge within B or C. A transmitted orbit centre suffers little change in its radius, even if it has collided many times within the constriction. Conversely a reflected orbit centre suffers a far larger change in its radius. This means that orbit centres in annuli A and B tend to be mixed by passage through a constriction while those in C remain, to a good approximation, independent.

3. Electron current and an effective particle picture

3.1. Procedure

Skipping electrons will orbit around an antidot, and thus constitute a circular current flow. It is necessary next to work out how much current is flowing in each of the three annular regions A, B and C. Calculation of this requires knowledge of both the electron occupancy and angular velocity of each orbit.

3.2. Occupancy of an orbit centre

Consider two areas A_1 and $A_2 = 2A_1$ of orbit centres in an infinite two-dimensional electron gas (hereafter denoted 2DEG). There will correspondingly be twice as many electrons with their orbit centres in A_2 than in A_1. However this simple proportionality does not hold near the boundary of a 2DEG.

Consider an infinitesimal area $\mathrm{d}A$ at a distance r from an antidot centre. If $r < R - r_c$ then there will be no electrons with orbit centres in $\mathrm{d}A$. If $r > R + r_c$ then there will be the same number as for an infinite 2DEG. For $R - r_c < r < R + r_c$ the number of electrons will be a function of r, namely $n_0 w(r)\mathrm{d}A$ (here n_0 is the electron sheet density in the reservoir). A suitable candidate for $w(r)$ is the fraction of a cyclotron orbit completed between successive collisions with the antidot. This choice preserves the total number of electrons when the B field is altered.

3.3. Current density at radius r

It is simple to define a time-averaged angular velocity $\dot{\phi}(r)$ for an orbit centre. The skipping frequency for an electron with its centre at radius r is $\omega_c/(2\pi w(r))$ and therefore

$$\dot{\phi}(r) = \frac{\omega_c}{2\pi}\frac{\phi(r)}{w(r)}.$$

The current density for orbit centres at radius r is then given by

$$j(r) = en_0 w(r) r\dot{\phi}(r) = en_0 \frac{\omega_c}{2\pi} r\phi(r). \tag{2}$$

This can then be integrated over the appropriate ranges to yield the current in each annulus.

3.4. Effective particle picture

It will be found later that it is sometimes inconvenient to use a centre angular velocity dependent upon r. It is easy instead to introduce a system of effective particles that orbit the antidot with an angular velocity independent of r but which have the same current density as the electron system. These particles have angular velocity $\dot{\phi} = \langle\dot{\phi}(r)\rangle$ = mean orbit centre angular velocity. They thus have a current density given by

$$n(r) = n_0 \frac{\omega_c}{2\pi} \frac{\phi(r)}{\langle\dot{\phi}(r)\rangle}. \tag{3}$$

3.5. Results for annular currents

In the experiments reported in I, the antidot arrays subjected to magnetotransport measurements had lattice spacings of $a = 800$, 1000, 2000 nm. Of particular interest are those of $a = 800$ nm, for which the antidot radius was estimated as $R = 300 \rightarrow 360$ nm. Figure 4 shows the results for annular current as a function of cyclotron radius for radii of 330 and 360nm. The current in annulus C, I_C shows little dependence on r_c, whereas I_A and I_B both increase with r_c as would be expected. The graphs also show the expected decrease in I_C due to a reduction in the constriction width. These field-dependent currents will be used as a base ingredient within the antidot array conductance treatment which follows in the next section.

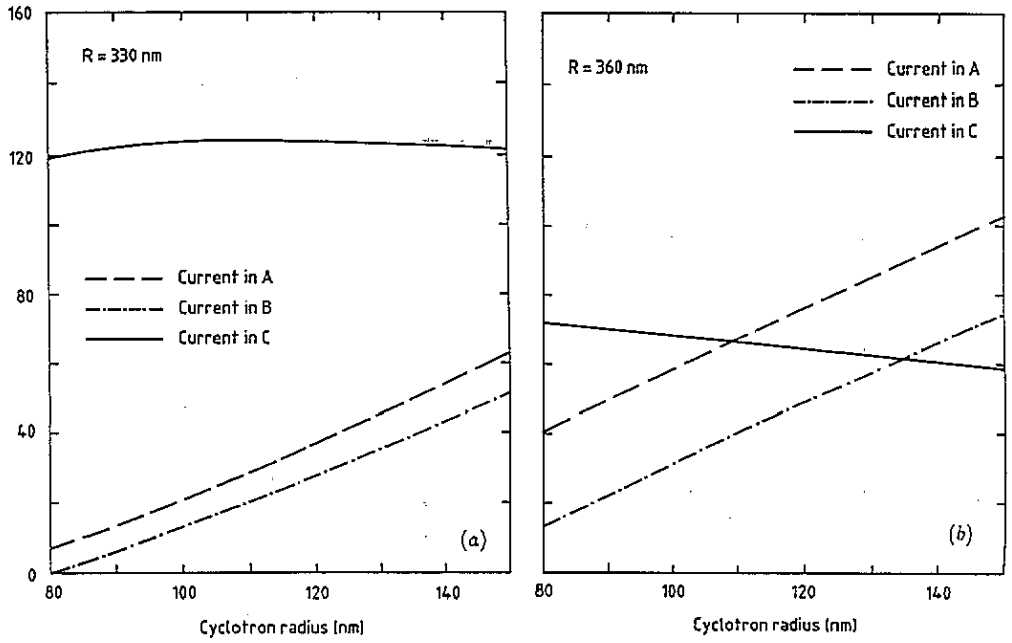

Figure 4. Circulating current in the three annuli A, B and C as a function of cyclotron radius, for (*a*) $R = 330$ nm and (*b*) $R = 360$ nm.

4. Application to the conductivity of an antidot lattice

To obtain the conductivity of the antidot lattice requires further consideration of the effect on the skipping electrons of scattering by impurities. This scattering is important because it provides a mechanism for the population of electrons in different skipping orbits and in the reservoir to come to equilibrium.

It is possible for a magnetic field to localize a reservoir electron in a region of space free of impurities, and so dramatically lengthen its scattering lifetime. However, skipping electrons are not localized in the same way, and so their lifetime is approximately the same as for electrons in zero field τ.

The low-scattering regime is particularly interesting, because here the mean free path of the electrons becomes large compared to the size of the lattice. The electrons then follow a random walk, passing from reservoir to reservoir. As discussed in section 4.1 below, these orbits give the dominant contribution to the conductivity in this regime.

We only calculate the linear response of the antidot lattice and so all quantities are evaluated in zero field.

4.1. Low-scattering regime

In this case $\langle\dot{\phi}(r)\tau\rangle \gg 1$, and an electron is very unlikely to be scattered between two successive constrictions. Because the orbit centres in annulus C are independent of those in A and B there are two separate contributions to the conductivity.

4.1.1. Contribution from orbit centres in C. These orbit centres are always transmitted and therefore merely circle a single antidot, passing through neighbouring reservoirs. Suppose that these reservoirs have slightly different electron densities. The current in annulus C will then be appropriate to some mean of these densities. In reservoirs of slightly higher density there will be a slight excess of electrons scattered into C and in reservoirs of lower density there will be a slight excess scattered out. This will give a net current flow between the reservoirs.

Figure 5 shows such a situation with a density gradient in the x direction. Consider a small element of area, $r\,\mathrm{d}r\,\mathrm{d}\phi$ in annulus C. This element will orbit the antidot with period $T(r) = 2\pi/\dot{\phi}(r)$ and will contain a density of centres given by

$$(n_0 + n(\phi))\,\omega(r) r\,\mathrm{d}r\,\mathrm{d}\phi$$

where $n(\phi)$ is to be found. If the point $\phi = 0$ is defined to be at the bottom of annulus C as shown in figure 5, then $n(\phi)$ will vary between two limits $n_u = n(\pi)$ and $n_l = -n_u = n(0)$. The rate of scattering into the element is proportional to $1/\tau$ and we have the equations

$$\dot{n}(\phi) = \left(\tfrac{1}{2}\delta n_0 - n(\phi)\right)(1/\tau) \qquad 0 < \phi < \pi$$

$$\dot{n}(\phi) = \left(\tfrac{1}{2} - \delta n_0 - n(\phi)\right)(1/\tau) \qquad \pi < \phi < 2\pi.$$

These equations can be solved to give

$$n_u = \frac{\delta n_0}{2}\tanh\left(\frac{T(r)}{4\tau}\right).$$

The time-average current carried in the x direction by this element is

$$\mathrm{d}^2 I_x = (n_u - n_l)\frac{1}{T(r)}\omega(r) r\,\mathrm{d}r\,\mathrm{d}\phi$$

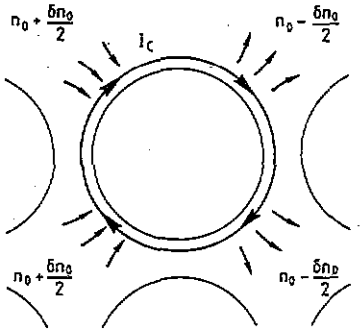

Figure 5. The contribution to the conductivity in the low-scattering regime from electrons in annulus C. The electrons circle an antidot, passing through reservoirs of different electron density. In reservoirs with density $n_0 + \delta n_0/2$ there is a slight excess of electrons scattered into the annulus C. Correspondingly there is a slight excess scattered out of C in reservoirs with density $n_0 - \delta n_0/2$.

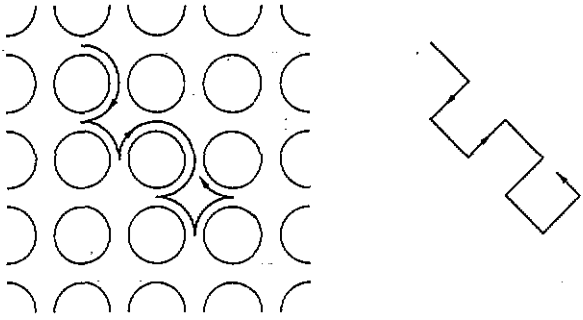

Figure 6. A typical path of an effective particle diffusing through the antidot lattice in the low-scattering regime. To the right is shown the corresponding 2D random walk.

which can be integrated to give

$$I_x = e\,\delta n_0 \int_{R-r_c}^{r_b} \dot{\phi}(r) \tanh\left(\frac{\pi}{2\dot{\phi}(r)\tau}\right) \omega(r)\,\mathrm{d}r. \tag{4}$$

In addition to I_x there will be a current in the y direction, which arises because more electrons are scattered into the element in the range $0 < \phi < \pi/2$ than in the range $\pi/2 < \phi < \pi$. This current is easily shown to be

$$I_y = e\,\delta n_0 \int_{R-r_c}^{r_b} \dot{\phi}(r) \tanh\left(\frac{\pi}{2\dot{\phi}(r)\tau}\right) \tanh\left(\frac{\pi}{4\dot{\phi}(r)\tau}\right) \omega(r)\,\mathrm{d}r. \tag{5}$$

In the low-scattering limit the tanh functions can be expanded to first order and the conductivity matrix can be deduced from (4) and (5). The result is

$$\sigma_{xx}^{c} = e\rho(\tfrac{1}{2}\pi)\frac{1}{\langle\dot{\phi}\rangle_c \tau} I_C^0 \tag{6}$$

$$\sigma_{yx}^{c} \approx (\tfrac{1}{4}\pi)\frac{1}{\langle\dot{\phi}\rangle_c \tau}\sigma_{xx}^{c} \tag{7}$$

where ρ is the zero field density of states in the reservoir, $\langle\dot{\phi}\rangle_c$ is the mean angular velocity of centres in annulus C, and $I_C^0 = I_C/n_0$.

4.1.2. Contribution from A and B. Consider an electron scattered into a skipping orbit with its centre in A or B. This electron will pass through many constrictions before being scattered again. At each constriction the orbit centre is sometimes transmitted and sometimes reflected. Its path will look like a 2D correlated random walk. An example is shown in figure 6.

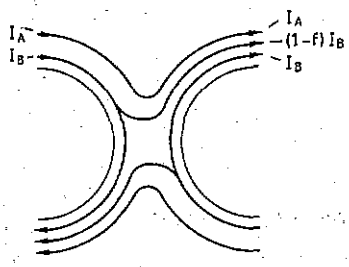

Figure 7. The transmission and reflection of currents at a constriction. The current in annulus C, I_c, is omitted for clarity. All of the current I_A is reflected, while a fraction f of I_B is transmitted and $(1-f)$ reflected.

This is where the effective particle picture is of use. These particles will also follow a random walk, but with the advantage that the time taken for each step is the same. This random walk still has the following complications. (i) The probabilities of transmission and reflection (turning left or right) are not equal. (ii) If the particle is transmitted then it has an enhanced probability of being transmitted again at the next constriction. This arises because a transmitted centre must emerge in annulus B.

The second point implies a correlation between successive steps which makes the walk non-trivial. Interacting walk problems of this type can be treated by mapping to equivalent Ising chains (Metha 1986) or by the following procedures.

Consider a walk of $2N$ steps, labelling the steps in the manner $x_1, y_1, x_2, y_2 \ldots x_N, y_N$. Each step can take the value $+1$ or -1, depending on whether it is in the positive or negative direction. We shall treat this walk approximately by proceeding to calculate the average probability that the step x_{i+1} is parallel to the step x_i.

The probability that a transmitted effective particle is in annulus B is 1, whereas for a reflected particle it is

$$\frac{(1-f)I_B}{I_A+(1-f)I_B}.$$

Defining $P(T,R)$ as the probability of transmission given that the particle was last reflected, and defining $P(T,T)$ in a similar manner, we get

$$P(T,R)=\frac{f(1-f)I_B}{I_A+(1-f)I_B} \qquad P(T,T)=f.$$

We now use these probabilities to express the probability that the step x_{i+1} of the walk is parallel to the step x_i.

Suppose that the step x_i was a transmitted one. The required probability would then be equal to $P(R,T)[P(T,R)+P(T,T)]$. If the step x_i was a reflected one then the required probability would be equal to $P(T,R)[P(R,R)+P(R,T)]$. Now let p_t be the average fraction of steps that are transmitted (see figure 7):

$$p_t=\frac{fI_B}{I_A+I_B}.$$

This then allows the definition of the average probability p_{for} that x_{i+1} is parallel to x_i

$$p_{for}=p_tP(R,T)[P(T,R)+P(T,T)]+(1-p_t)P(T,R)[P(R,R)+P(R,T)]$$

$$p_{for}=f(1-f)\frac{2I_B}{I_A+I_B}.$$

The correlation function $\langle x_{i+1}x_i\rangle$ is then given in this approximation by $-\gamma = p_{\text{rev}} - p_{\text{for}}$. Similarly $\langle x_i y_i\rangle = 1 - 2p_t$. These can be iterated to give

$$\langle x_i x_{i+n}\rangle = (-\gamma)^n \tag{8}$$

$$\langle x_i y_{i+n}\rangle = (1-2p_t)(-\gamma)^n. \tag{9}$$

From these correlation functions the diffusion matrix can be calculated (see appendix). The result is

$$\mathbf{D} = \frac{\langle\dot{\phi}\rangle_{A+B}}{2\pi}\left(\frac{a^2}{2}\right)\left(\frac{1-\gamma}{1+\gamma}\right)\begin{pmatrix} 1 & (1-2p_t) \\ (1-2p_t) & 1 \end{pmatrix}.$$

The conductivity matrix can then be obtained using the Einstein relation, which gives

$$\sigma^{A+B} = e\rho\frac{1}{2}\left(\frac{1-\gamma}{1+\gamma}\right)I^0_{A+B}\begin{pmatrix} 1 & (1-2p_t) \\ (1-2p_t) & 1 \end{pmatrix}. \tag{10}$$

4.2. High-scattering regime

In this case $\langle\dot{\phi}(r)\rangle\tau \ll 1$, and an electron is very likely to be scattered as it moves between two successive constrictions. The current carried by skipping orbits entering a constriction will then be in equilibrium with the electron population in the reservoir. As the scattering increases the mean number of steps taken in a random walk of an effective particle decreases until eventually the concept of a random walk breaks down and (10) no longer holds.

The contribution to the conductivity from annular region C is easily determined from (4) and (5) by letting $\tau \to 0^+$. This gives

$$\sigma_c = e\rho I^0_c\begin{pmatrix} 1 & -1 \\ 1 & 1 \end{pmatrix}.$$

None of the centres in annulus A are transmitted and therefore A makes no contribution to the conductivity. In contrast a fraction f of the centres in B are transmitted and these contribute to σ. The total conductivity is therefore

$$\sigma = e\rho(I^0_C + fI^0_B)\begin{pmatrix} 1 & -1 \\ 1 & 1 \end{pmatrix}. \tag{11}$$

4.3. Results

The conductivity matrices given by (6), (7) and (10) can easily be numerically evaluated and inverted to obtain the resistivity of the lattice.

The result for the high-scattering case is shown in figure 8, where we have a taken the electron density to be $3.3 \times 10^{15}\,\text{m}^{-2}$ (comparable to the electronic densities reported in I), and performed the calculation for antidot radii of 300, 330, and 360 nm. As expected the resistivity rises as the constriction narrows. All of the graphs show a steady positive differential magnetoresistance (PMR). For the 330 and 360 nm graphs this PMR is quite small, which is a direct consequence of the small dependence of I_B on the B field. The upturn in the 360 nm graph occurs when $2r_c$ becomes less than the constriction width. At this point the annuli A and B disappear, and I_C has far greater B field dependence. The larger

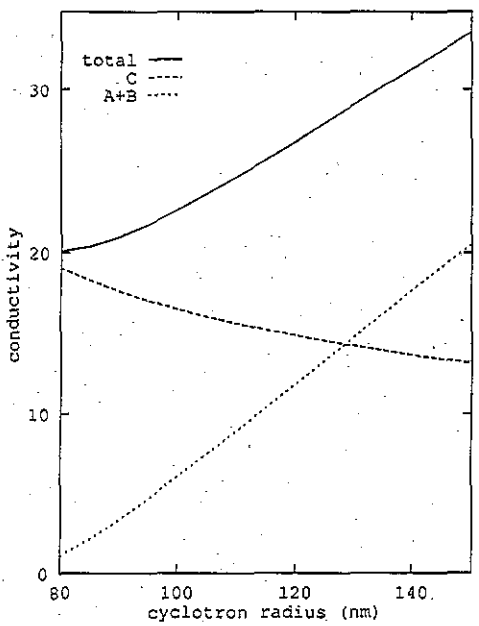

Figure 8. Longitudinal resistivity in the case of high scattering. The graphs are for three different antidot radii, 300, 330 and 360 nm. The electron density in the reservoir was taken to be $3.3 \times 10^{15}\,\mathrm{m}^{-2}$.

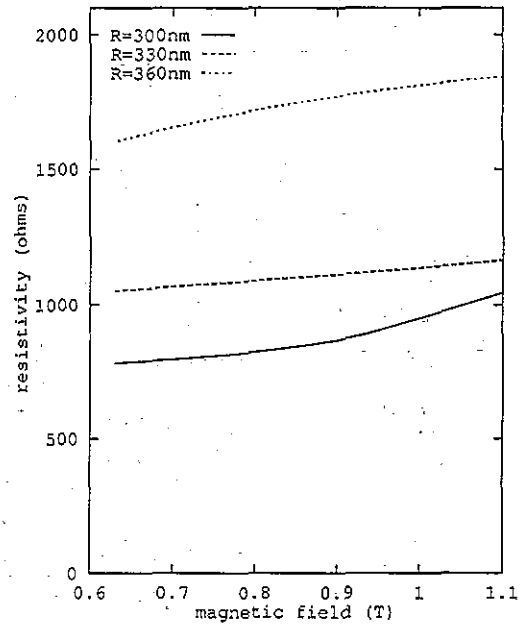

Figure 9. Longitudinal component of the conductivity in the low-scattering regime for an antidot radius of 330 nm and a scattering time $\tau = 24$ ps. The two lower lines show the separate contributions from annulus C and from annuli A and B.

PMR seen in the 360 nm graph is a consequence of the reduction of the size of annulus C with deceasing constriction width. A greater fraction of the conductivity then comes from electrons in annulus B, whose current I_B has greater dependence on magnetic field.

The results for the low-scattering case are shown in figures 9 and 10. The calculations were done for an electron sheet density of $3.3 \times 10^{15}\,\mathrm{m}^{-2}$ and antidot radii of 300, 330 and 360 nm. Figure 9 shows the two separate contributions to the conductivity from annulus C and annuli A and B, for the case $R = 330$ nm and $\tau = 24$ ps. This clearly shows the competition between σ_{A+B} which has a PMR and σ_C which exhibits negative differential magnetoresistance (NMR). The trend of the total conductivity is dominated by the random walk contribution and exhibits PMR. Figures 10(*a*) and (*b*) show the resistivity for the various antidot radii for the cases $\tau = 24$ ps and $\tau = 32$ ps respectively. Even though these are long scattering times they still only correspond to a mean number of steps in the walk of 6 and 8 respectively. Comparing the graphs to the high scattering case, there is far less dependence on antidot radius and a far greater dependence on magnetic field. This is a reflection of the dominating contribution of the random walk. In both graphs the line for $R = 300$ nm levels off as $2r_c$ approaches the constriction width l. As this limit is approached the annuli A and B become very small, and so does the number of particles performing a random walk. Annulus C dominates the conductivity leading to a leveling off of the resistivity. Once $2r_c$ becomes less than l, I_C once again develops a larger field dependence and the resistivity rises again.

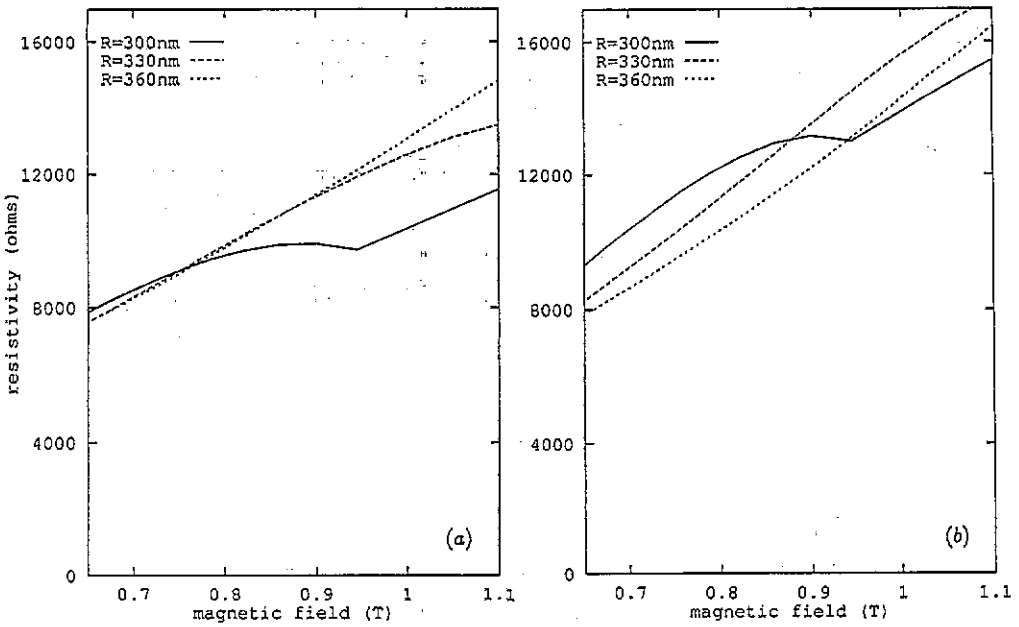

Figure 10. Longitudinal resistivity in the case of low scattering for various antidot radii. The electron density was taken to be $3.3 \times 10^{15}\,\mathrm{m}^{-2}$, and the scattering time τ as 24 ps in (*a*) and 32 ps in (*b*).

5. Conclusion

We have presented two mechanisms for conduction in an antidot lattice in the presence of a magnetic field. One involved scattering into and out of skipping orbits that were localized around a single antidot. The other involved orbits that pass through many reservoirs in the fashion of a random walk. The model used was a particularly simple one, with a perfect lattice of identical hard wall antidots. A more realistic model would need to include a softer potential. So long as the potential at the edge of an antidot remained steep, and that within the reservoir remained fairly flat, then the concept of skipping orbits would remain a good one. The qualitative aspects discussed in this paper would remain valid, but the details of the conductance calculations would be changed. An improved model would also have to take into account the effects of disorder, in terms of variation of both the lattice constant and antidot radius. Such disorder would most seriously effect the random walks. Any abnormally wide constrictions would tend to localize the paths to orbit around an antidot, while abnormally narrow constrictions would tend to localize them to orbit a reservoir. The disorder of the real lattices studied in I is small, however it can be non-negligible in certain situations. In particular it is responsible for a conduction threshold which occurs on varying the electron density in zero field.

When a comparison is made between the results in I and those presented here it is found that the lattices used were just inside the high scattering regime. The magnitude of the resistivity calculated here compares well with the values measured in I. However, whereas we predict a small PMR, the experiments showed a small NMR. Such discrepancies are not unexpected considering the simplicity of our model.

Our model breaks down at high fields, where quantum effects become important, and

also at very low magnetic fields. As the field is reduced the cyclotron radius increases until eventually there exist orbit centres that are within r_c of more than two antidots. The concept of a skipping orbit breaks down. Instead of considering the passage of an electron through a single constriction it is necessary to consider its path through the lattice as a whole (Weiss 1991). Even in a perfect lattice there will be chaotic orbits present (Fleischmann 1992, Berthold 1992). Disorder will then be very important. For example, any deviation in the shape of an antidot from a circle will change the angle of a reflected electron. While this will not dramatically effect the motion of a skipping electron, it will drastically effect the subsequent path of an electron in a low magnetic field.

Acknowledgments

We would like to thank Dr G Sundaram for helpful discussions and for supplying I prior to publication. One of us, RT, would like to thank Stephen T West for his aid with the computational work.

Appendix

In general, the diffusion matrix is given by

$$D = \int_0^\infty \langle v(t)v(0)\rangle \, \mathrm{d}t.$$

Define the vector r_i to be $\sqrt{a^2/2}(x_i, y_i)$. A random walk of an effective particle of length $2N$ steps is then uniquely specified by the vectors $r_1 \ldots r_N$. We can define a velocity $v_i = r_i/2T$, where $T = \pi/(2\langle\dot{\phi}\rangle_{A+B})$ is the time taken for one step. With these definitions the diffusion matrix becomes

$$D = \tfrac{1}{2}\langle v_1 v_1\rangle + \sum_{n=2}^{\infty}\langle v_n v_1\rangle$$

$$D = (1/4T)\langle r_1 r_1\rangle + \frac{1}{2T}\sum_{n=2}^{\infty}\langle r_n r_1\rangle.$$

We then have

$$D_{yx} = \frac{\langle\dot{\phi}\rangle_{A+B}}{2\pi}\left(\frac{a^2}{2}\right)\left(\langle y_1 x_1\rangle + \frac{1}{2}\sum_{n=1}^{\infty}\langle y_{n+1}x_1\rangle\right)$$

and

$$D_{xx} = \frac{\langle\dot{\phi}\rangle_{A+B}}{2\pi}\left(\frac{a^2}{2}\right)\left(\langle x_1 x_1\rangle + \frac{1}{2}\sum_{n=1}^{\infty}\langle x_{n+1}x_1\rangle\right).$$

References

Brey L *et al* 1989 *Phys. Rev.* B **40** 10647
Büttiker M 1981 *Phys. Rev.* B **38** 9375
Ensslin K and Petroff P M 1990 *Phys. Rev.* B **41** 12307
Fang H and Stiles P J 1990 *Phys. Rev.* B **41** 10171
Fleischman R *et al* 1992 *Phys. Rev. Lett.* **68** 1367
Ford C J B *et al* 1990 *Surf. Sci.* **229** 298
Halperin B 1982 *Phys. Rev.* B **25** 2185
Hansen W *et al* 1989 *Phys. Rev. Lett.* **62** 2168
Kern K *et al* 1991 *Phys. Rev. Lett.* **66** 1618
Kohn W 1962 *Phys. Rev.* **123** 1242
Kosevich A M and Lifshitz I M 1955 *Zh. Eksp. Theor. Fiz.* **29** 743 (Engl. transl. 1956 *Sov. Phys.–JETP* **2** 648)
Lorke A *et al* 1990 *Phys. Rev. Lett.* **64** 2559
—— *et al* 1992 *Phys. Rev.* B **46** 12845
Maksym P A and Chakraborty T 1990 *Phys. Rev. Lett.* **65** 108
Metha A and Stinchcombe R B 1990 *J. Phys. A: Math. Gen.* **19** 2155
Prange R E and Nee T W 1968 *Phys. Rev.* **168** 779
Que W and Kirczenow G 1988 *Phys. Rev.* B **38** 3614
Reed M A *et al* 1986 *Phys. Rev. Lett.* **60** 535
Rourkes M L *et al* 1987 *Phys. Rev. Lett.* **59** 3011
Sikorski Ch and Merkt U 1989 *Phys. Rev. Lett.* **62** 2168
Smith T P *et al* 1988 *Phys. Rev.* B **38** 2172
Stinchcombe R B 1974 *J. Phys. C: Solid State Phys.* **7** 4277
Sundaram G 1992 *DPhil. thesis* Oxford University
Takahara J *et al* 1991 *Japan. J. App. Phys.* **30** 3250
Weiss D 1991 *Phys. Rev. Lett.* **66** 2790